Photoassisted activation of persulfate by $Cu_2(OH)_2CO_3$ for the degradation of tetracycline hydrochloride

S. J. Li[a,*], E. Pang[b], W. J. Zhao[c]
[a]*Institute of Traffic Engineering, Shanxi Vocational University of Engineering Science and Technology, Taiyuan 030619, China*
[b]*Research Group of New Energy Materials and Devices, North University of China, Taiyuan 030051, China*
[c]*School of Science, Yanshan University, Qinhuangdao 066004, China*

$Cu_2(OH)_2CO_3$ (cupric carbonate basic, CCB) is a common copper-based semiconductor compound that can absorb the visible light due to its suitable bandgap structure. Here, CCB was synthesized by a one-pot hydrothermal strategy. The catalyst exhibited excellent activation activity of persulfate (PS) supported by visible light irradiation and can degrade tetracycline hydrochloride (TCH) over a wide pH range from 3.0 to 10.0. Under the condition of 0.1 g/L catalyst and 2 mM PS, the removal rate of TCH (30 mg/L) reached 96% after 60 min of visible light irradiation. Coexisting anions (Cl^-, HCO_3^-, SO_4^{2-}) had little effect on the TCH degradation. The synergistic effects of CCB combined with PS and visible light were beneficial for the separation of photogenerated hole-electrons and the generation of more free radicals. Electron paramagnetic resonance (EPR) experiments and quenching experiments show that $HO^·$ and h^+ are the predominant species in the catalytic reaction. Thus, this study proposes a promising approach using the CCB/PS/Vis system for wastewater remediation.

(Received November 19, 2023; February 20, 2024)

Keywords: Photocatalysis, Persulfate, Advanced oxidation process, Tetracycline

1. Introduction

Sulfate radical ($SO_4^{·-}$)-based advanced oxidation processes (SR-AOPs) has aroused great concern as a promising technology in sewage treatment, due to its high oxidation potential (2.5-3.1 V) over a wide pH range and longer half-life (30-40 μs) [1-4]. $SO_4^{·-}$ is commonly generated through the activation of PS or peroxymonosulfate (PMS) by heat, microwave, ultrasound, UV, catalyst and combination of two or more activation methods [5-12]. Among these strategies, catalyst-coupled visible light activation methods have emerged as a promising approach due to their ease of operation and use of inexhaustible solar energy [1, 13-16]. Specifically, the catalyst was excited by visible light to generate photoinduced electrons, which can subsequently activate PS or PMS to produce $SO_4^{·-}$. Liu et al. [1] supported Cu atoms on carbon nitride matrix, and the catalyst showed excellent degradation of TCH performance using PS coupling with LED light

* Corresponding author: lishijia@sxgkd.edu.cn
https://doi.org/10.15251/DJNB.2024.191.309

sources. Li et al. [14] Synthesized a N and Fe codoped carbon dots (N, Fe-CDs) by a one-pot hydrothermal method, PMS can be activated by a new Fe(III)/Fe(II) cycling system for aminopyrine degradation under visible light irradiation.

CCB is a common copper based semiconductor compound that can absorb the visible light due to its suitable bandgap structure [17]. Thus，the CCB and its compound find extensive applications in the domain of photocatalytic hydrogen production, hydrogen peroxide production, artificial nitrogen fixation cocatalyst and dye degradation [17-23]. He et al. [17] fabricated $Cu_2(OH)_2CO_3/TiO_2$ by a simple precipitation method, which was applied as an efficient co-catalyst in photocatalytic hydrogen evolution reaction. Li et al. [22] reported that a full-spectrum response $Cu_2(OH)_2CO_3/g\text{-}C_3N_4$ can be applied in photocatalytic H_2O_2 production. Liang et al. [21] prepared an N vacancy-doped $g\text{-}C_3N_4/Cu_2(OH)_2CO_3$ heterojunction catalyst with a superior broad-spectrum-driven N_2 photofixation ability. Furthermore, $Cu_2(OH)PO_4$ (libethenite) exhibited strong energy absorption in the NIR region and was an effective photocatalyst for the oxidation of 2,4-dichlorophenol (2,4-DCP) in aqueous solution under NIR light irradiation [24]. PS could also be activated by $Cu_4SO_4(OH)_6$ (brochantite) for the degradation of tetracycline hydrochloride (TC-H) [25]. To the best of our knowledge, no previous studies have reported the utilization of CCB to activate PS for the degradation of organic contaminants.

As a common antibiotic, TCH is widely used in disease treatment, aquaculture and animal husbandry due to its ease of synthesis, low processing cost and excellent antibacterial properties [26-29]. TCH has a stable chemical structure that does not readily oxidise or biodegrade. Residual TCH will contaminate the natural water environment, leading to bacterial resistance and significant fluctuations in the environmental microbiota [27]. Traditional wastewater treatment plants cannot effectively remove TCH residues, so it is necessary to find an efficient and convenient method to remove TCH residues in water.

In this paper, CCB was synthesized by hydrothermal method using copper nitrate and urea as feedstock. The morphology, phase structure and photoelectrochemical properties of CCB were revealed through various characterizations. In particular, to the best of our knowledge, the CCB was used for the first time to activate PS for the degradation of TCH under visible light irradiation. Besides, the effects of catalyst amount, PS amount, initial pH value and inorganic anions on the TCH degradation reaction were also investigated. EPR experiments and quenching experiments identified the main active species. Moreover, the possible mechanism of PS activation was proposed.

2. Experimental

2.1. Materials and chemicals

Methanol (MeOH, 99.9%), 5,5-dimethyl-1-pyrroline N-oxide (DMPO, 97%), tert-butyl alcohol (TBA, AR) were purchased from Macklin Biochemical Co., Ltd. (shanghai, China). Copper nitrate ($Cu(NO_3)_2{\cdot}3H_2O$, AR), urea (AR), tetracycline hydrochloride (TCH), sodium persulfate (PS, AR), ethylenediaminetetraacetic acid disodium salt dihydrate (EDTA-2Na-$2H_2O$, AR), sodium hydroxide (NaOH, AR), sulfuric acid (H_2SO_4), Nafion were obtained from Aladdin Biochemical co., Ltd. (shanghai, China). Deionised water was used throughout the experiment.

2.2. Synthesis of catalytic materials

CCB were prepared through hydrothermal strategy. 2 mmol $Cu(NO_3)_2 \cdot 3H_2O$ and 8 mmol urea were added into 30 mL of deionised water and dispersed by ultrasound for 30 min. The mixture was then placed in a Teflon-lined stainless steel autoclave at 120 ℃ for 12 hours and cooled naturally. The obtained precipitates were washed 3 times with water and ethanol and dried at 80 ℃ for 12 hours.

2.3. Characterisation of the catalysts

The morphology of the samples was observed by scanning electron microscope (SEM, Hitach, Japan), transmission electron microscope (TEM, FEI Tecnai, Holland). The phase of the composition was analysed by X-ray diffraction (XRD, Bruker, Germany). The XPS patterns were obtained by an X-ray photoelectron spectrometer (XPS, Shimadzu Kratos AXIS, Japan). Electrochemical experiments were performed using an Electrochemical Workstation (CHI 660E, China). the UV-Vis diffuse reflectance spectra (DRS) was carried out on UV-2550 (Shimadzu, Japan). The zeta potential of samples was acquired on a zeta potential analyser (Malvern, UK). The EPR signals were captured by a electron paramagnetic resonance spectrometer (Bruker, Germany).

2.4. Catalytic activity evaluation

The degradation of TCH evaluated the catalytic performance of the sample. Typically, 5.0 mg of catalyst was added to 50 ml of aqueous TCH solution (30 mg/L), and stirred in the dark condition for 30 min to achieve adsorption-desorption equilibrium. A defined amount of PS was then added to the suspension, which was immediately irradiated under a 300 W Xenon lamp with a 420 nm cut-off filter. At a regular intervals, 1 mL of reaction solution mixed with 1 mLof methanol was filtered through a 0.22 μm filter and the mixture were analyzed by high-performance liquid chromatography (HPLC, Shimadzu).

The HPLC system was equipped with an Shim-pack GIS-C18 column (250 mm×4.6 mm, 5 μm) and UV-Vis diode array detector at 356 nm. The eluent consisted of 0.2 % formic acid solution and methanol (75:25, v:v) with a flowing rate of 1.0 mL/min.

3. Results and discussion

3.1. Characterization of the catalyst

The XRD patterns of the sample before and after the reaction are shown in Fig.1a. The six peaks at 14.8°, 17.6°, 24.1°, 31.2°, 32.2°, and 35.6° are highly matched with the lattice planes at (020), (120), (220), (201), (211), and (240) of monoclinic cupric carbonate basic (PDF No. 41-1390)[19]. The XRD pattern of the used CCB did not change, indicating that the CCB have a stable crystal structure. The morphology of CCB was observed by SEM in Fig.S1. CCB reveal its irregular lamellar structures with some smooth surfaces and the thickness of 200 nm. Fig.1b display the TEM images of CCB, which showed an irregular polygonal 2D structure, consistent with the SEM image. Furthermore, the HRTEM image of crystal region confirmed that the interplanar spacing is about 0.278nm (Fig.1c and d), which is consistent with the (211) lattice plane of CCB. Beside, XPS technique was also carried out to further determine the specific surface

composition and elemental status. The survey scan (Fig.S2a) confirmed the presence of Cu, O, C elements. The Cu2p spectrum (Fig.S2b) exhibited the peaks of 933.9 eV and 954.1 eV corresponding to the Cu^{2+} [20]. The above results indicate that CCB has been successfully prepared in this work.

The optical properties of CCB were measured using UV-Vis diffuse reflectance spectra (DRS). As shown in Fig.S3, the spectra show an apparent absorption edge at about 462 nm. which is consistent with previous research [20]. Moreover, the absorption spectra exbibit a high absorption in Visible region, where the absorption band located at 700-800 nm can be attributed to the d-d transition of Cu(Ⅱ)[17]. In particular, the absorption region of CCB extends almost into the near infrared region.

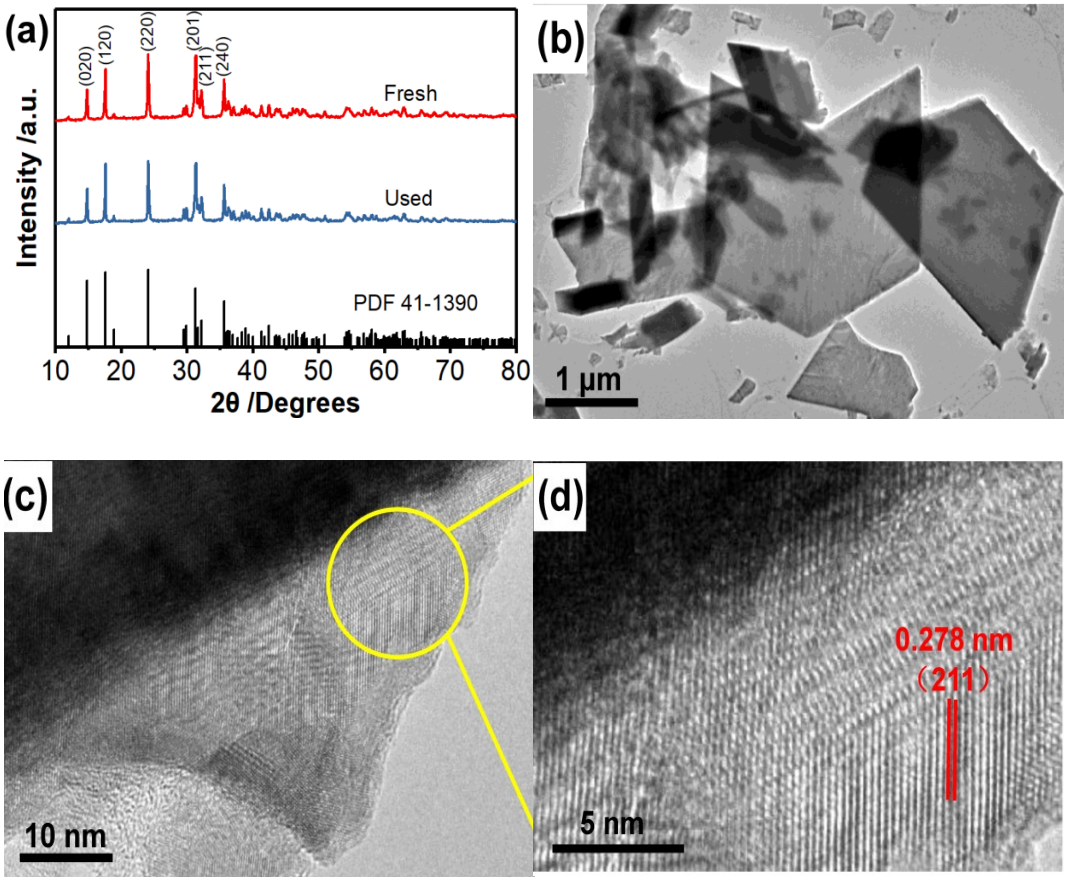

Fig. 1. (a) XRD patterns of the fresh and used CCB. (b)TEM and (c, d) HRTEM images of CCB.

3.2. Catalytic performance of the materials

The catalytic performance of different systems was evaluated by the degradation of TCH solution. As shown in Fig. 2a, the PS/Vis system had almost no effect on TCH removal, indicating that PS does not generate free radicals to eliminate TCH under visible light irradiation. In the CCB/Vis system, the degradation rate of TCH at 60 min was 11.8%, which is obviously caused by adsorption. without light irradiation, 33.9% of TCH can be eliminated with the CCB/PS system within 60 min. This shows that CCB can slightly activate PS to produce free radicals to remove

TCH without light irradiation. Especially, 96% of TCH was removed by CCB in the co-presence of PS and visible light. The reaction rates of all the systems are shown in Figure 2b. Obviously, the degradation rate of CCB/PS/Vis was much higher than other systems, indicating that CCB, light and PS play a synergistic role in the degradation of TCH. Therefore, it can be concluded that visible light-assisted activation of PS by CCB can greatly improve the degradation efficiency of TCH.

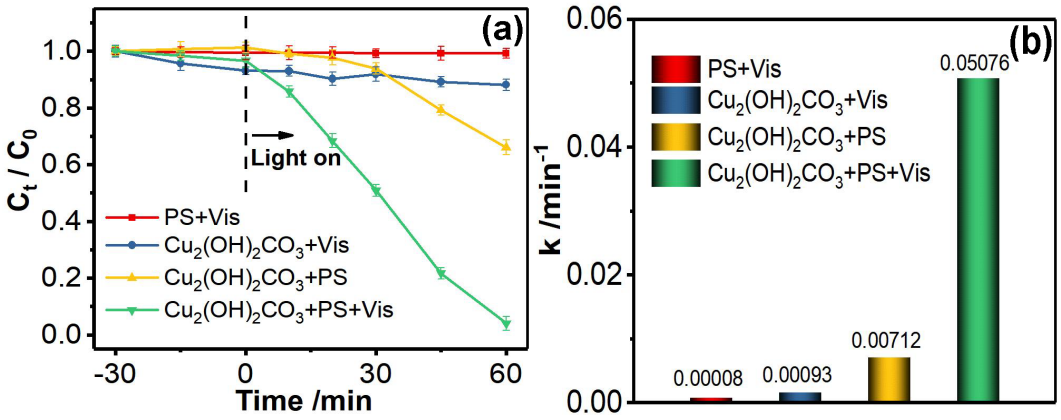

Fig. 2. (a) Degradation of TCH under different systems and (b) their corresponding reaction kinetics. Expeimental conditions: [catalyst]=0.1 g/L, [PS]=2 mM, [TCH]=30 mg/L, pH 6.8.

The effects of catalyst dosage, PS dosage, pH and co-existing anions on TCH degradation were also investigated. Fig.3a showed that the removal rate gradually increased as the catalyst dosage increased from 0.02 to 0.2 g/L, which was attributed to the more active sites and photogenerated carriers for the activation of PS. Furthermore, Fig.3b displayed that the removal efficiency of TCH increased as the PS concentration increased from 0.2 mM to 1 mM. When the PS concentration was further increased to 2 mM, the TCH removal efficiency remained unchanged. This is probably due to the fact that excessive PS can cause quenching of free radicals [30]. In addition, a certain amount of catalyst can only activate PS at a certain reaction rate, and the catalyst may also be a limiting factor at higher PS concentrations.

As shown in Fig.3c, the CCB/PS/Vis system exhibited excellent degradation efficiency under acidic and neutral conditions. The TCH removal rates were 100%, 100% and 96% at pH=3.0, 5.0 and 6.8 respectively. However, the TCH degradation rate was slightly decreased at pH=10, and 81.5% of TCH was removed within 60 min. This is due to the fact that under alkaline conditions, TCH existed mainly in the TC^{2-} and TCH^{-} ionic states, while, CCB was negatively charged at pH=3-10 (Fig.S4), so the electrostatic repulsion between the catalyst and TCH created a barrier and inhibited the catalytic reaction. Various coexisting anions have always been present in practical wastewater, which may be react with the free radicals to form other radicals with weak oxidising ability and inhibit the TCH degradation. Here, the effects of Cl^{-}, HCO_3^{-}, NO_3^{-}, and SO_4^{2-} on TCH degradation were evaluated. It has been reported that Cl^{-} and HCO_3^{-} can quench $SO_4^{\cdot-}$ and $HO^{\cdot}$ and inhibit the removal efficiency of organic pollutants [31]. Notably, as shown in Fig.3d, these ions had almost no significant effect on TCH removal except for NO_3^{-} ions, suggesting that the activation of PS via the non-radical pathway is involved in these processes.

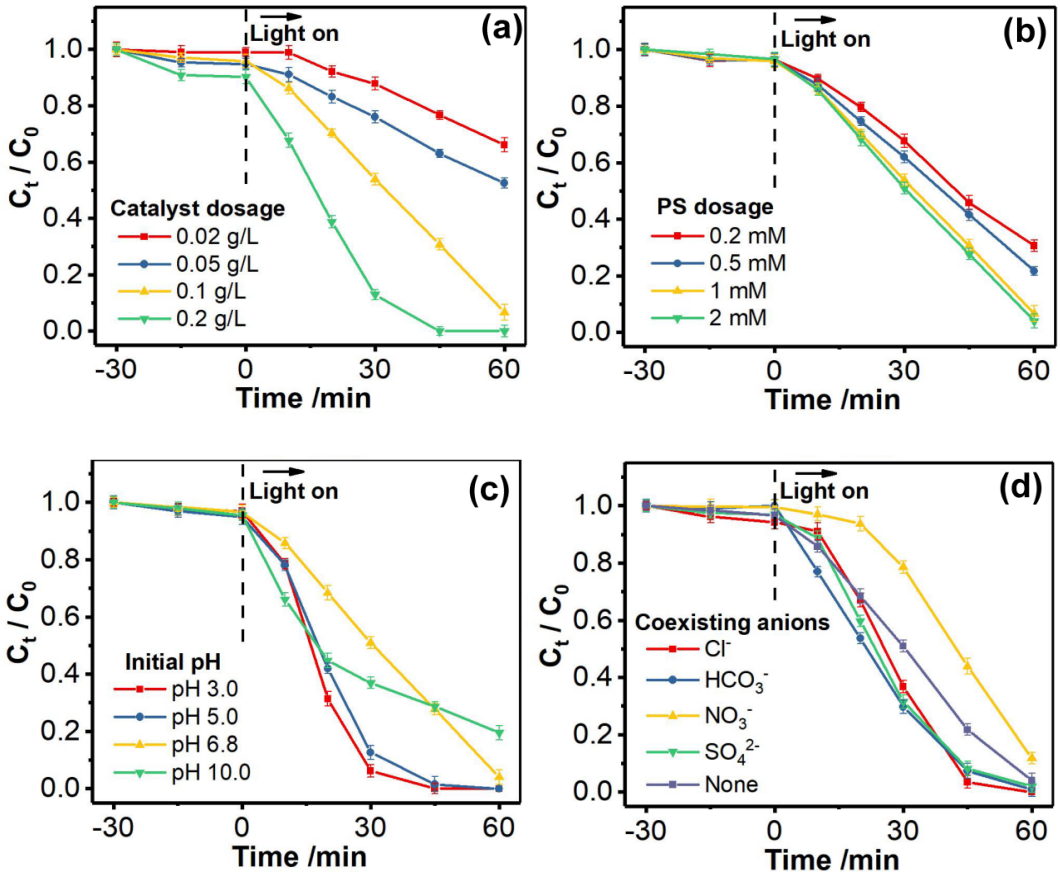

Fig. 3. Effect of (a) catalyst dosage (Expeimental conditions: [PS]=1 mM, [TCH]=30 mg/L); (b) PS dosage (Expeimental conditions: [catalyst]=0.1 g/L, [TCH]=30 mg/L); (c) initial pH (Expeimental conditions: [catalyst]=0.1 g/L, [PS]=2 mM, [TCH]=30 mg/L); (d) co-existing anions (Expeimental conditions: [Cl^-]=[HCO_3^-]=[NO_3^-]=[SO_4^{2-}]=5 mM, [catalyst]=0.1 g/L, [PS]=2 mM, [TCH]=30 mg/L) on the degradation of TCH by CBB/PS/Vis.

Repeated TCH removal experiments were carried out to investigate the durability of the catalyst. As shown in Fig. S5, the removal rates of TCH ranged from 96% to 77.2%, and the XRD pattern of the used catalyst was consistent with that of the fresh catalyst (Fig. 1a), indicating that the structure was hardly changed in the reaction.

3.3. Catalytic mechanisms of CCB/PS/Vis system

Previous studies have confirmed that $SO_4^{\cdot-}$ and $HO^{\cdot}$ can be produced by PS activation, which organic pollutants can be removed by these free radicals. Meanwhile, non-radical pathways for PS activation have also received much attention in recent studies. It is necessary to fully investigate the influence of two pathways in this degradation system. EPR analysis was firstly performed for identification the type of free radicals. DMPO is used as trapping agents for $SO_4^{\cdot-}$ and $HO^{\cdot}$, which can form DMPO-$SO_4^{\cdot-}$ and DMPO-$HO^{\cdot}$ Adducts. Fig.4a shows that no obvious EPR signals were detected in CCB/Vis, indicating that CCB cannot produce free radicals without PS. Meanwhile the signals of DMPO-$SO_4^{\cdot-}$ and DMPO-$HO^{\cdot}$ were observed in the CCB/PS system,

indicating that CCB can slightly activate PS to produce free radicals under dark conditions. Notably, obvious signals of DMPO-$HO^{\cdot}$ and DMPO-$SO_4^{\cdot-}$ were detected in the CCB/PS/Vis system, indicating that visible light boosted the generation of free radicals. The results reveal that the visible light can greatly facilitate the activation of PS by CCB, which is beneficial for the generation of free radicals.

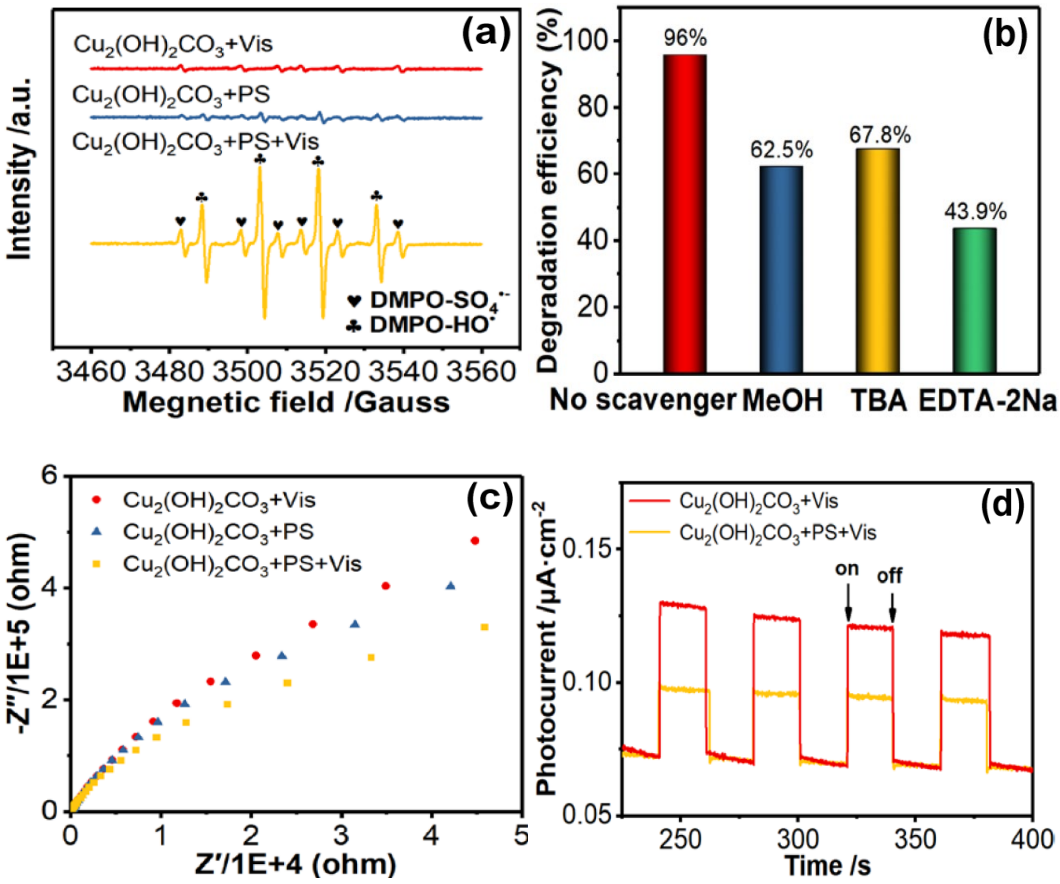

Fig. 4. (a) EPR spectra of DMPO-$SO_4^{\cdot-}$ and DMPO-$HO^{\cdot}$ adducts. (Expeimental conditions: [catalyst]=0.1 g/L, [PS]=2 mM, [DMPO]=0.1 M). (b) Comparison of the removal rates with different scavengers. (Expeimental conditions: [catalyst]=0.1 g/L, [PS]=2 mM, [TCH]=30 mg/L, [MeOH]=[TBA]=500 mM, [EDTA-2Na]=1 mM). (c) Transient photocurrent responses of different systems. (d) EIS Nyquist plots of different systems.

Photogenerated carriers play a crucial role in PS activation. Hence, the transfer efficiency of photogenerated carriers was evaluated using electrochemical impedance spectra (EIS) (Fig.4c). The smaller arc radius indicates lower charge transfer resistance and better transfer efficiency [15]. The CCB/PS/Vis system appears to have the smallest arc radius compared to other systems, indicating the best electronic conductivity. The results showed that the coupling of PS and visible light could effectively accelerate the interfacial electron-hole separation and transfer of CCB, which greatly improved the degradation efficiency of TCH. Furthermore, the transient photocurrent response was shown in Figure.4d. The CCB can generate stable photocurrents under

visible light irradiation, however, the photocurrent decreased with the addition of PS, further indicating that PS can efficiently trap the photogenerated electrons in the CCB/PS/Vis system. In conclusion, the multiple synergistic interaction between PS and visible light effectively inhibits the recombination of photogenerated holes with electrons and promotes the generation of more free radicals.

Subsequently, radical trapping experiments were carried out to evaluate the role of free radicals in the CCB/PS/Vis system (Fig. 4b). MeOH was used to quench $SO_4^{\cdot-}$ and $HO^{\cdot}$, and TBA was added to trap $HO^{\cdot}$ [32]. the removal rates of TCH were 62.5% and 67.8% after the addition of MeOH and TBA respectively, indicating that the inhibitory effect of MeOH was slightly greater than than that of TBA. The results suggested that $HO^{\cdot}$ plays a more important role than $SO_4^{\cdot-}$ in the degradation of TCH. Furthermore, EDTA-2Na was used as trapping agents for photogenerated holes (h^+) [15]. Particularly, the removal rate of TCH was only 43.9% after the addition of EDTA-2Na, implying that h^+ was also involved in the catalytic reaction. Combined with the effects of coexisting anion experiments and radical trapping experiments, it can be concluded that h^+ and $HO^{\cdot}$ are the main active species for the catalytic degradation of TCH in the system.

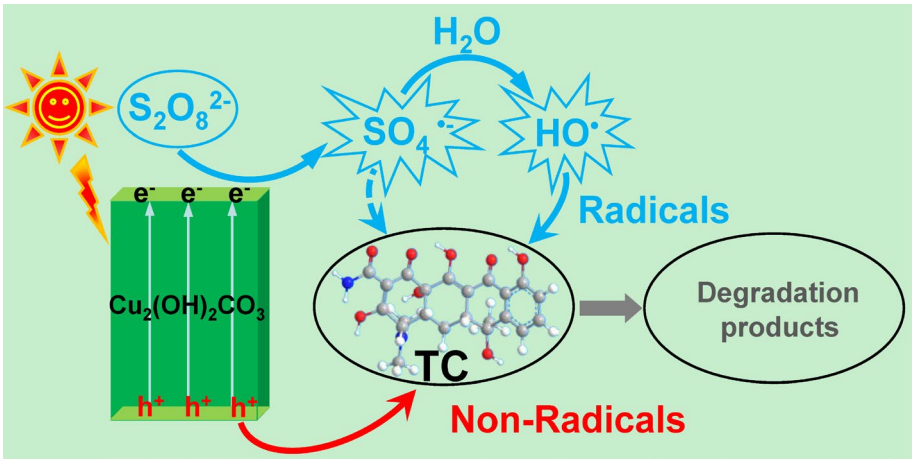

Fig. 5. The proposed mechanism of TCH degradation in CBB/PS/Vis.

The possible mechanism for TCH degradation by CCB/PS/Vis system is proposed in Fig.5. CCB can be excited to generate the electron-hole pairs under visible light, which PS could serve as electron traps to enhance the separation efficiency of the photogenerated carrier (Eq. (1)). The $S_2O_8^{2-}$ adsorbed on the catalysts was directly activated by the photogenerated electron to produce $SO_4^{\cdot-}$ (Eq. (2)). Subsequently, the $SO_4^{\cdot-}$ can also combine with H_2O to form $HO^{\cdot}$(Eq. (3)). Beside, TCH could also be decomposed by the photogenerated hole via a non-radical pathway. In summary, $SO_4^{\cdot-}$, $HO^{\cdot}$, and h^+ all play an important roles for TCH degradation in CBB/PS/Vis system(Eq. (4)).

$$CCB + h\nu \rightarrow h^+ + e^- \quad (1)$$

$$S_2O_8^{2-} + e^- \rightarrow SO_4^{2-} + SO_4^{\cdot-} \quad (2)$$

$$SO_4^{\cdot-} + H_2O \rightarrow HO^{\cdot} + SO_4^{2-} + H^+ \quad (3)$$

$$h^+/HO^{\cdot}/SO_4^{\cdot-} + TCH \rightarrow products \quad (4)$$

4. Conclusion

In conclusion, CBB was prepared by a facile one-pot hydrothermal method, and exhibited superior PS activation activity under visible light. The removal rate of TCH reached 96% within 60 min in the CCB/PS/Vis system. The synergistic effect between CCB, PS and light played a pivotal roles in the degradation of TCH. PS can act as an electron trap to boost more $SO_4^{\cdot-}$ and $HO^{\cdot}$ radicals. $HO^{\cdot}$, and h^+ were the predominant species for TCH degradation. CCB also exhibited excellent chemical stability and recyclability, as well as adaptability to a wide pH range. Moreover, the system had a strong anti-interference ability, which anions (Cl^-, HCO_3^-, SO_4^{2-}) had little effect on the degradation process. This study provided a new approach for the activation of PS by CCB coupling with visible light in the degradation of organic pollutants.

References

[1] J. Liu, H. He, Z. Shen, H.H. Wang, W. Li, J. Hazard Mater. 429, 128398 (2022); https://doi.org/10.1016/j.jhazmat.2022.128398.
[2] J. Wang, S. Wang, Chem. Eng. J. 334, 1502 (2018); https://doi.org/10.1016/j.cej.2017.11.059.
[3] W.-D. Oh, Z. Dong, T.-T. Lim, Appl. Catal. B-Enviro. 194, 169 (2016); https://doi.org/10.1016/j.apcatb.2016.04.003.
[4] S. Wacławek, H.V. Lutze, K. Grübel, V.V.T. Padil, M. Černík, D.D. Dionysiou, Chem. Eng. J. 330, 44 (2017); https://doi.org/10.1016/j.cej.2017.07.132.
[5] W.S. Chen, Y.C. Shih, Chemosphere 239, 124686 (2020); https://doi.org/10.1016/j.chemosphere.2019.124686.
[6] Y. Pan, Y. Zhang, M. Zhou, J. Cai, Y. Tian, Chem. Eng. J. 361, 908 (2019); https://doi.org/10.1016/j.cej.2018.12.135.
[7] X. Ao, W. Sun, S. Li, C. Yang, C. Li, Z. Lu, Chem. Eng. J. 361, 1053 (2019); https://doi.org/10.1016/j.cej.2018.12.133.
[8] Z. Xie, Y. Feng, F. Wang, D. Chen, Q. Zhang, Y. Zeng, W. Lv, G. Liu, Appl. Catal. B-Enviro. 229, 96 (2018); https://doi.org/10.1016/j.apcatb.2018.02.011.
[9] S. Norzaee, M. Taghavi, B. Djahed, F. Kord Mostafapour, J. Environ. Manage. 215, 316 (2018); https://doi.org/10.1016/j.jenvman.2018.03.038.
[10] W. Chu, D. Li, N. Gao, M.R. Templeton, C. Tan, Y. Gao, Water Res. 72, 340 (2015); https://doi.org/10.1016/j.watres.2014.09.019.
[11] C. Qi, X. Liu, C. Lin, X. Zhang, J. Ma, H. Tan, W. Ye, Chem. Eng. J. 249, 6 (2014); https://doi.org/10.1016/j.cej.2014.03.086.
[12] T. Zhang, Y. Yang, X. Li, H. Yu, N. Wang, H. Li, P. Du, Y. Jiang, X. Fan, Z. Zhou, Sep. Purif. Technol. 239, 116537 (2020); https://doi.org/10.1016/j.seppur.2020.116537.
[13] X. Jiang, K. Xiao, Z. Liu, W. Xu, F. Liang, S. Mo, X. Wu, J. Beiyuan, Sep. Purif. Technol. 296, 121328 (2022); https://doi.org/10.1016/j.seppur.2022.121328.

[14] Q. Li, H. Lu, X. Wang, Z. Hong, Z. Fu, X. Liu, J. Zhou, Chem. Eng. J. 443, 136473 (2022); https://doi.org/10.1016/j.cej.2022.136473.
[15] H. Chen, X. Zhang, L. Jiang, X. Yuan, J. Liang, J. Zhang, H. Yu, W. Chu, Z. Wu, H. Li, Y. Li, Sep. Purif. Technol. 272, 118947 (2021); https://doi.org/10.1016/j.seppur.2021.118947.
[16] T. Guo, L. Jiang, H. Huang, Y. Li, X. Wu, G. Zhang, J. Hazard Mater. 416, 125838 (2021); https://doi.org/10.1016/j.jhazmat.2021.125838 .
[17] Z. He, J. Fu, B. Cheng, J. Yu, S. Cao, Appl. Catal. B-Enviro. 205, 104 (2017); https://doi.org/10.1016/j.apcatb.2016.12.031.
[18] D. Chen, X. Wang, X. Zhang, W. Wang, Y. Xu, Y. Zhang, G. Qian, Int. J. Hydrogen Energ. 45(46), 24697 (2020); https://doi.org/10.1016/j.ijhydene.2020.06.225.
[19] Y. Liu, X. Wu, H. Lv, Y. Cao, H. Ren, Dalton T. 48(4), 1217 (2019); https://doi.org/10.1039/c8dt03579b.
[20] Y. Liu, H. Ren, H. Lv, Z. Gong, Y. Cao, Appl. Surf. Sci. 484, 1061 (2019); https://doi.org/10.1016/j.apsusc.2019.04.148.
[21] H. Liang, L. Fang, S. Hu, New J. Chem. 43(30), 12094 (2019); https://doi.org/10.1039/c9nj01306g.
[22] Z. Li, N. Xiong, G. Gu, Dalton T. 48(1), 182 (2019); https://doi.org/10.1039/c8dt04081h.
[23] H. Xu, D. Dai, S. Li, L. Ge, Y. Gao, Dalton T. 47(2), 348 (2018); https://doi.org/10.1039/c7dt04096b.
[24] G. Wang, B. Huang, X. Ma, Z. Wang, X. Qin, X. Zhang, Y. Dai, M.H. Whangbo, Angew. Chem. Int. Ed. 52(18), 4810 (2013); https://doi.org/10.1002/anie.201301306.
[25] W. Dong, T. Cai, Y. Liu, L. Wang, H. Chen, W. Zeng, J. Li, W. Li, J. Colloid Interf. Sci. 585, 400 (2021); https://doi.org/10.1016/j.jcis.2020.11.106.
[26] F. Ahmad, D. Zhu, J. Sun, Environ. Sci. Eur. 33(1) (2021); https://doi.org/10.1186/s12302-021-00505-y.
[27] G. Gopal, S.A. Alex, N. Chandrasekaran, A. Mukherjee, RSC Adv. 10(45), 27081 (2020); https://doi.org/10.1039/d0ra04264a.
[28] Y. Zhang, J. Zhou, X. Chen, L. Wang, W. Cai, Chem. Eng. J. 369, 745 (2019); https://doi.org/10.1016/j.cej.2019.03.108.
[29] L. Niu, G. Zhang, G. Xian, Z. Ren, T. Wei, Q. Li, Y. Zhang, Z. Zou, Sep. Purif. Technol. 259, 118156 (2021); https://doi.org/10.1016/j.seppur.2020.118156.
[30] Q. Zhong, Q. Lin, R. Huang, H. Fu, X. Zhang, H. Luo, R. Xiao, Chem. Eng. J. 380, 122608 (2020); https://doi.org/10.1016/j.cej.2019.122608.
[31] J. Wang, S. Wang, Chem. Eng. J. 411, 128392 (2021); https://doi.org/10.1016/j.cej.2020.128392.
[32] R. Li, H. Hu, Y. Ma, X. Liu, L. Zhang, S. Zhou, B. Deng, H. Lin, H. Zhang, J. of Clean. Prod. 276, 124246 (2020); https://doi.org/10.1016/j.jclepro.2020.124246.